

Structural Characterization of Ru–Bleomycin Complexes by Resonance Raman, Circular Dichroism, and NMR Spectroscopy

Barbara Mouzopoulou,^{†,‡} Henryk Kozlowski,^{†,§} Nickos Katsaros,[‡] and Arlette Garnier-Suillerot^{*,†}

Laboratoire de Physicochimie Biomoléculaire et Cellulaire, Université Paris Nord, Bobigny 93017, France, Institute of Physical Chemistry, NCSR “Demokritos”, Paraskevi Attikis, Greece, and Faculty of Chemistry, University of Wrocław, Wrocław, Poland

Received October 4, 2000

A series of spectroscopic techniques including absorption and CD spectra, resonance Raman spectra, and ¹H NMR as well as electrospray mass spectrometry have shown that Ru(II) ion binds to bleomycin, forming an equimolar complex, similarly to Fe(II), i.e., via the secondary amine nitrogen, the pyrimidine ring nitrogen, the deprotonated peptide bond nitrogen of the histydy residue, and the histidine imidazole nitrogen, which are bound in the equatorial positions, and the α -amino nitrogen of β -aminoalanine, which coordinates in the apical position above pH 7. The reaction of Ru(II)–BLM with O₂, H₂O₂, or PhIO leads to formation of the oxy species in which only one oxygen atom is bound to metal ion. According to our data, the reaction of Ru(II)–BLM complex with oxygen species leads to different product than that suggested for Fe(II)–BLM. The formation of the BLM–Ru–O–Ru–BLM dimeric unit, similar to that found for sterically unhindered Ru porphyrins, seems to be the most likely.

Introduction

The bleomycins are a family of glycopeptide antibiotics isolated from the culture medium of *Streptomyces verticillus* as their copper chelates by Umezawa et al.¹ Bleomycin A2 (BLM, Figure 1), which differs from other naturally occurring bleomycins only in the cationic C-terminus, is the major component (70%) of the anticancer drug Bleomycin, which is used for the treatment of Hodgkin's lymphoma, carcinomas of the skin, head, and neck, and testicular cancers.^{2–4}

Bleomycin A2 is thought to exert its biological effects through DNA binding and degradation, a process that is metal ion and oxygen dependent.^{5–13} It cleaves double-strand DNA selectively at (5'-GC or 5'-GT sites by minor groove C4'-H abstraction and subsequent fragmentation of the deoxyribose backbone.⁴ Although iron appears to be the most effective bleomycin cofactors, other metals bind strongly to bleomycin,^{14–20} and

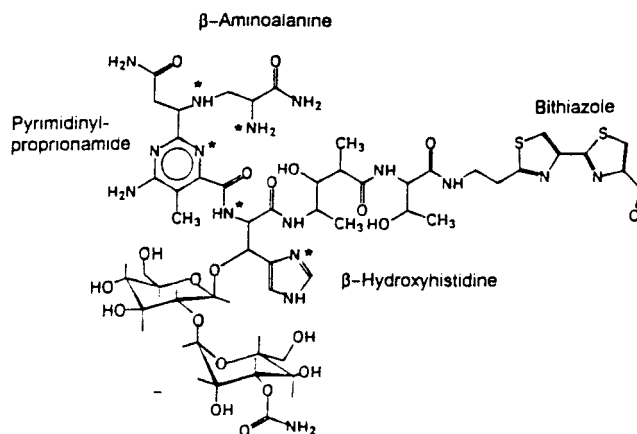


Figure 1. Bleomycin. The potential metal-binding ligands are shown in bold for clarity.

some can facilitate DNA cleavage by mechanisms less well understood than that of iron.²¹

Extensive structural, chemical, and biophysical studies^{3,4} have shown that the most likely metal binding sites are centered in the N-terminus. The most likely donor system was determined from the X-ray structure of Cu(II) 5-coordinate, square-pyramidal complex with P3A, an N-terminal fragment of BLM,²² lacking the bithiazole and sugar moieties, and other simplified BLM mimic ligands.²³ According to these model studies, the binding donor set consists of five nitrogens, i.e.,

* Corresponding author. Tel: 33 1 48 38 77 48. Fax: 33 1 48 38 77 77. E-mail: garnier@lpsc.jussieu.fr.

[†] Université Paris Nord.

[‡] Institute of Physical Chemistry.

[§] University of Wrocław.

- Umezawa, H.; Maeda, K.; Takeuchi, T.; Okamai, Y. *J. Antibiot.* **1966**, *19*, 200–209.
- Lazo, J. S.; Chabner, B. A. *Cancer Chemotherapy and Biotherapy: Principles and Practice*; Chabner, A. B., Longo, D. L., Eds.; Lippincott-Raven: Philadelphia, 1996; pp 379–393.
- Umezawa, H.; Maeda, K.; Takeuchi, T.; Okami, Y. *J. Antibiot.* **1966**, *19*, 200–209.
- Boger, D. L.; Cai, H. *Angew. Chem.* **1999**, *38*, 448–476.
- Ishida, R.; Takahashi, T. *Biochim. Biophys. Res. Commun.* **1975**, *66*, 1432–1438.
- Sausville, E. A.; Peisach, J.; Horwitz, S. B. *Biochim. Biophys. Res. Commun.* **1976**, *73*, 814–822.
- Sausville, E. A.; Stein, R. W.; Peisach, J.; Horwitz, S. B. *Biochemistry* **1978**, *17*, 2740–2746.
- D'Andrea, A. D.; Haseltine, W. A. *Proc. Natl. Acad. Sci.* **1978**, *75*, 3608–3612.

(9) Takeshita, M.; Grollman, A. P.; Ohtubo, E.; Ohtsubo, H. *Proc. Natl. Acad. Sci.* **1978**, *75*, 5983–5987.

(10) Povirk, L. F. *Biochemistry* **1979**, *18*, 3989–3995.

(11) Burger, R. M.; Peisach, J.; Horwitz, S. B. *J. Biol. Chem.* **1981**, *256*, 11636–11644.

(12) Sam, J. W.; Tang, X.-J.; Peisach, J. *J. Am. Chem. Soc.* **1994**, *116*, 5250–5256.

the secondary amine nitrogen, pyrimidine ring nitrogen, deprotonated peptide nitrogen of histidine residue, and histidine imidazole nitrogen, which coordinate as the basal planar donor, and the α -amino nitrogen of β -aminoalanine, which coordinates as the axial donor; the metal site has fundamentally a square-pyramidal structure with four chelate rings of 5–5–5–6 ring members. No crystal structure exists for a metal complex of BLM, and there is some controversy concerning the ligation of BLM to metal ions. This concerns mainly the axial ligand coordination, which could be the primary amine of the β -aminoalanine fragment and/or the carbamoyl substituent on the mannose sugar. Although the involvement of the former donor is more likely, some controversy about the axial binding site may still exist.⁴ Concerning metal ion binding domain, various spectroscopic techniques usually give a partial answer about the metallobleomycin structure or the involved donor set. The lack of an X-ray structure of a particular BLM–metal complex makes NMR a powerful tool in solving the metal ion–BLM complex structure, although other techniques such as resonance Raman,²⁴ circular dichroism,^{14–16,18,19} or electrospray mass spectrometry^{12–25} could be extremely useful in describing details of the system studied, e.g., some specific structural features of activated bleomycin.¹² Actually, the metal complex of BLM, despite the lack of a heme prosthetic group, resembles several metalloporphyrins, and metal–bleomycin complexes are intermediate between ordinary complexes and metalloporphyrins.^{26–27}

Since ruthenium is a fifth-row transition metal in the homologous series with iron, the Ru ion has been considered as a suitable substitute for the Fe ion, despite the chemical differences between Ru and Fe atoms. However, the studies on the ruthenium–bleomycin system are very limited: in the 1980s, γ -emitting Ruthenium-103 was used as a label to evaluate Ru–BLM tissue distribution,²⁸ and Ru(II)–BLM complex was shown to cleave DNA in the presence of UV light and O₂.²⁹ However, neither of these works reported the data allowing evaluation of the metal binding sites of the complexes formed. Gray et al.³⁰ described the chemical and biological properties of pentaammineruthenium–bleomycin complex using ¹H NMR

and differential pulse voltammetric data. In the latter case, Ru(III) formed monodentate bonds to the imidazole or the pyrimidine moieties of BLM.

With the Ru–BLM system and its interactions with O₂ being poorly understood, on one hand, and Ru(II) complexes containing N-donor ligands being able to undergo facile electron transfer to molecular oxygen, on the other hand, we have undertaken a systematic study of the interaction of BLM with ruthenium in the absence and in the presence of oxygen. *cis*- and *trans*-RuCl₂(DMSO)₄ were used as source of Ru(II), mainly because they are both very soluble and stable in aqueous solution. Their aqueous chemistry as well as their interactions with small ligands is well-documented. Our data show that in the absence of oxygen, a 1:1 Ru^{II}BLM species is formed. This complex reacts with molecular oxygen, with H₂O₂, and with PhIO, yielding a robust and kinetically inert complex that may more likely be formulated as a μ -oxo ruthenium–BLM complex: [Ru^{IV}BLM]₂O. In conclusion, the Ru–BLM complexes seem to function quite differently from the Fe–BLM complexes, with more similarities to the Ru–porphyrins.

Experimental Section

Products. Bleomycin A2 (BLM) was a generous gift of Nippon Kayaku and was used without further purification. *cis*-RuCl₂(DMSO)₄ complex was obtained as described earlier.³¹ Ruthenium *cis*-isomer was used in the synthesis of *trans*-complex according to the procedure given in the literature.³²

Circular Dichroism and Absorption Spectroscopy. Absorption spectra were recorded on a Cary 219 and circular dichroism (CD) spectra on a Jobin-Yvon-Spex model CD 6 dichrograph. The dichrograph was calibrated with a standard solution of epiandrosterone (3.4×10^{-3} M) in a 1 cm cell ($\Delta\epsilon = 3.3 \text{ M}^{-1} \text{ cm}^{-1}$ at 304 nm). The CD spectra were recorded in 0.5 and 0.1 cm cells in the 320–650 and 220–650 nm range, respectively. Results are expressed as ϵ (absorption) and $\Delta\epsilon = \epsilon_L - \epsilon_R$. Equimolar solutions of 10^{-3} M were used for the measurements.

NMR Spectroscopy. ¹H NMR spectra were recorded on a AM BRUKER Aspect 300, at 500 MHz. COSY magnitude spectra were recorded in D₂O with a data matrix 2048 (t_2) \times 256 (t_1) data points. The spectral width was 5000 Hz in D₂O. Zero-filling in t_1 was employed to yield a final absorptive spectrum of 2048 \times 1024 data points. Complexes II, II', III, and III' were prepared as described, lyophilized, and redissolved in D₂O with a final concentration of 5×10^{-3} M for all samples. For ¹H NMR, the solvent peak (HDO) signal was used as an internal reference ($d = 4.80$ at 25 °C). The solvent peak was suppressed by selective irradiation ($d1=1.2s$, $S3 = 25L$) prior to acquisition.

Resonance Raman Spectroscopy. Resonance Raman spectra were recorded at room temperature on a T64000 triple spectrograph (Jobin Yvon) with a CCD detection system and a premono stage working in subtractive mode. Scattered light was dispersed by a spectral stage equipped with a 600 or 1200 grooves/mm grating. All spectra were excited with the 488-nm line of an argon ion laser (Model 2017, Spectra-Physics) with a light power at sample of ca. 100 mW. The spectral slit width was set to 5 cm^{-1} . Each spectrum was accumulated 20 or 40 times with 30 s acquisition time, resulting in a total acquisition time of 10 or 20 min per spectrum. Raman shifts were calibrated by means of toluene with a wavenumber scale accuracy $\pm 1 \text{ cm}^{-1}$. No sample changes were detected during the measurements. Baseline correction was performed for all spectra to remove residual fluorescence background. The concentration used for the Raman measurements was 10^{-3} M for all samples in H₂O and D₂O.

- (13) Burger, R. M.; Tian, G.; Drlica, K. *J. Am. Chem. Soc.* **1995**, *117*, 1167–1168.
 (14) Albertini, J.-P.; Garnier-Suillerot, A. *Biochem. Biophys. Res. Commun.* **1981**, *102*, 499–506.
 (15) Albertini, J.-P.; Garnier-Suillerot, A.; Tosi, L. *Biochem. Biophys. Res. Commun.* **1982**, *29*, 557–563.
 (16) Albertini, J.-P.; Garnier-Suillerot, A. *Biochemistry* **1982**, *21*, 6777–6782.
 (17) Chang, C.-H.; Meares, C. F. *Biochemistry* **1982**, *21*, 6332–6337.
 (18) Albertini, J.-P.; Garnier-Suillerot, A. *Biochemistry* **1984**, *23*, 47–53.
 (19) Albertini, J.-P.; Garnier-Suillerot, A. *Inorg. Chem.* **1986**, *25*, 1216–1221.
 (20) Sucheck, S. J.; Ellena, J. F.; Hecht, S. M. *J. Am. Chem. Soc.* **1998**, *120*, 7450–7460.
 (21) Petering, D. H.; Byrnes, R. W.; Antholine, W. E. *Chem. Biol. Interact.* **1990**, *73*, 133–141.
 (22) Itaka, Y.; Nakamura, H.; Nakatani, T.; Muraoka, Y.; Fujii, A.; Takita, T.; Umezawa, H. *J. Antibiot.* **1978**, *31*, 1070–1073.
 (23) Kimura, E. H.; Kurosaki, Y.; Kurogi, M.; Shionoya, H.; Shiro, M. *Inorg. Chem.* **1992**, *31*, 4314–4321.
 (24) Takahashi, S.; Sam, J. W.; Peisach, J.; Rousseau, D. L. *J. Am. Chem. Soc.* **1994**, *116*, 4408–4413.
 (25) Sam, J. W.; Tang, X.-J.; Magliozzo, R. S.; Peisach, J. *J. Am. Chem. Soc.* **1995**, *117*, 1012–1018.
 (26) Loeb, K. E.; Zaleski, J. M.; Westre, T. E.; Guajardo, R. J.; Mascharak, P. K.; Hedman, B.; Hodgson, K. O.; Solomon, E. I. *J. Am. Chem. Soc.* **1995**, *117*, 4545–4561.
 (27) Loeb, K. E.; Zaleski, J. M.; Hess, C. D.; Hecht, S. M.; Solomon, E. I. *J. Am. Chem. Soc.* **1998**, *120*, 1249–1259.
 (28) Stern, P. H.; Halpern, S. E.; Hagan, Ph. L.; Howell, S. B. *J. Natl. Cancer Inst.* **1981**, *66*, 807–811.
 (29) Subramanian, R.; Meares, C. F. *Biochem. Biophys. Res. Commun.* **1985**, *133*, 1145–1150.

- (30) Gray, H. B.; Margalit, R.; Clarke, J. M.; Podbielski, L. *Chem. Biol. Inter.* **1986**, *59*, 231–245.
 (31) Evans, E. I. P.; Spencer, A.; Wilkinson, G. *J. Chem. Soc. Dalton Trans.* **1973**, 204–210.
 (32) Alessio, E.; Mestroni, G.; Nardin, G.; Attia, W. M.; Calligaris, G.; Sava, G.; Zorzet, S. *Inorg. Chem.* **1988**, *27*, 4099–4106.

Table 1. Absorption and CD Spectral Features of BLM and Ru–BLM Complexes II, II', III, and III'

proposed assignment		$\pi \rightarrow \pi^*$ pyrimidine	$\pi \rightarrow \pi^*$ imidazole	$\pi \rightarrow \pi^*$ bithiazole	$n \rightarrow \pi^*$ 4'-amino pyrimidine	metal–ligand charge transfer	
free BLM pH 4	λ_M	~240 sh	~240 sh	287	310		
	(ϵ_M)	(37 000)	(20 000)	(14 000)	(sh)		
	$\Delta\epsilon_M$	(-4.6)	(-2)	(1)	(-0.1)		
free BLM pH 7	λ_M	~240 sh	~240 sh	287	310		
	(ϵ_M)	(37 000)	(20 000)	(14 000)	(sh)		
	$\Delta\epsilon_M$	(-2)	(-1)	(+0.5)			
II pH 4	λ_M			290		~400	
	(ϵ_M)			(17 000)		(2200)	
	$\Delta\epsilon_M$	233	266 sh	297		400	444
II' pH 7	λ_M	(-4)	(-0.5)	(2.4)		(1.5)	(-0.5)
	(ϵ_M)			(15 000)			
	$\Delta\epsilon_M$	241		297		335 sh	406
III pH 4	λ_M	(-1.3)		(+2.6)		(+1.2)	(+0.9)
	(ϵ_M)			(13 000)			~380 sh
	$\Delta\epsilon_M$	230	261	296	317	336	(2600)
III' pH 7	λ_M	(-4)	(-2)	(-0.5)	(0.8)	(0.8)	(1.3)
	(ϵ_M)			(11 000)			~400 sh
	$\Delta\epsilon_M$	230	252	290		346	(4000)
	λ_M	(-2.6)	(-2)	(-1)		(0.7)	(1.7)
	(ϵ_M)						~490 sh
	$\Delta\epsilon_M$						(2200)
	λ_M						412
	(ϵ_M)						498
	$\Delta\epsilon_M$						(1.3)
	λ_M						~400 sh
	(ϵ_M)						(4000)
	$\Delta\epsilon_M$						(2400)
	λ_M						383
	(ϵ_M)						526
	$\Delta\epsilon_M$						(1.3)

Electrospray Mass Spectrometry. All mass spectra were obtained using a Finnigan-MAT TSQ 7000 mass spectrometer. The electrospray needle was 4.5 kV. The solvent used was H₂O and the flow rate 3.00 mL/min. The capillary temperature was 2000 °C and the N₂ flow rate 50 psi.

Results

Ru(II)–BLM Complex Formation in the Absence of Oxygen. BLM was dissolved in H₂O in the absence or in the presence 0.1 M NaCl and degassed with N₂ or Ar for several minutes. Then (always under Ar/N₂) *cis/trans*-RuCl₂(DMSO)₄ was added at 1:1 molar ratio (pH 4.0) and the solution obtained was boiled under Ar/N₂ at 90 °C. The same reaction was also performed at different ratios of Ru:BLM equal to 2:1 and 1:2. All reactions between BLM and Ru complexes were monitored using absorption and CD spectroscopy. In the absence of oxygen, a first “intermediary” complex was formed in water solutions containing 0.1 M NaCl. This entity can be obtained using either *cis*- or *trans*-RuCl₂(DMSO)₄ as the starting material. However, its formation was faster when using the *cis*- than the *trans*-Ru compound (~5 min versus ~15 min at 90 °C). Actually, upon dissolution in water *cis*-RuCl₂(DMSO)₄ immediately releases the O-bonded DMSO to form the neutral monoqua species.³³ In the second step, slow dissociation of chloride ion results in formation of the *cis*-diaqua complex. The *trans*-RuCl₂(DMSO)₄ complex, when dissolved in water, releases relatively rapidly two DMSO molecules to give a complex with two water molecules being in *cis*-position to each other and in *trans*-position to two S-bonded DMSO ligands.³³ The second step is once again the slow dissociation of the first Cl⁻. The chloride dissociation for both isomers is almost complete in the absence of NaCl, while it is completely suppressed in 0.1 M NaCl solution. It is usually assumed that coordinated water molecule is of labile nature; thus, in solutions containing 0.15 and 0.01 M Cl⁻, *trans*-Ru(II) isomer forms derivatives with two and three labile positions, respectively, while the *cis*-isomer has one or two labile positions, respectively. It has been shown for the *cis*-isomer that binding of the first N-ligand favors the dissociation of one DMSO *cis* to it. Therefore, BLM introduced

into the solution containing any of the mentioned above isomers will react with Ru(II) starting at the water-bound sites, with the *trans*-complex being more readily coordinating to BLM than the other one. According to our spectroscopic data, this “intermediary” complex I was actually a mixture of several species, and we will not here enter into the details of its characterization.

Still in the absence of oxygen after additional heating (2 h at 90 °C), a second complex was formed, hereafter named II or II', depending on whether the preparation was performed at pH 4.0 or 7.0. The reaction was monitored by visible absorption and CD spectroscopy, and heating was continued until the reaction was judged complete by UV/vis spectroscopy. The compounds were yellow, and according to CD and vis spectroscopy, the stoichiometry was 1:1. In the absence of oxygen, both complexes can be conserved for months.

Absorption and CD Features of Complexes II and II'. The absorption and CD spectra of free BLM is characterized by the presence of four absorption and CD bands at wavelengths lower than 320 nm, which have been assigned to the $\pi \rightarrow \pi^*$ transition of pyrimidine at 230 nm, imidazole at 237 nm, and bithiazole at 290 nm and to the $n \rightarrow \pi^*$ transition of 4'-aminopyrimidine at 310 nm.³⁴ The CD spectrum of free BLM is slightly dependent on pH: at pH 4.0, when most of imidazole is protonated, the amplitude of the CD signal at ~240 nm is twice that observed at pH 7.0, when imidazole is deprotonated (see Table 1).

The CD spectral patterns of complexes II and II' were characterized mostly by the appearance of new CD bands at ~340, ~400, and ~440 nm, while absorption spectra showed usually one broad band centered around 400 nm ($\epsilon \sim 2000$) (Figure 2). These bands were most likely of charge-transfer origin. On the other hand, the band due to the bithiazole at 290 nm was still seen in the two spectra with a positive signal. Also

- (33) Mestroni, G. E.; Alessio, M.; Calligaris, W. M.; Attia, F.; Quadrioglio, S.; Cauci, G.; Sava, S.; Zorzet, S.; Pacor, C.; Monti-Bragadin, M.; Tamaro, A.; Dolzani, L. *Progress. Clin. Biochem.* **1989**, *10*, 71–76.
 (34) Chien, M.; Grollmann, A. P.; Horwitz, S. B. *Biochemistry* **1977**, *16*, 3641–3647.

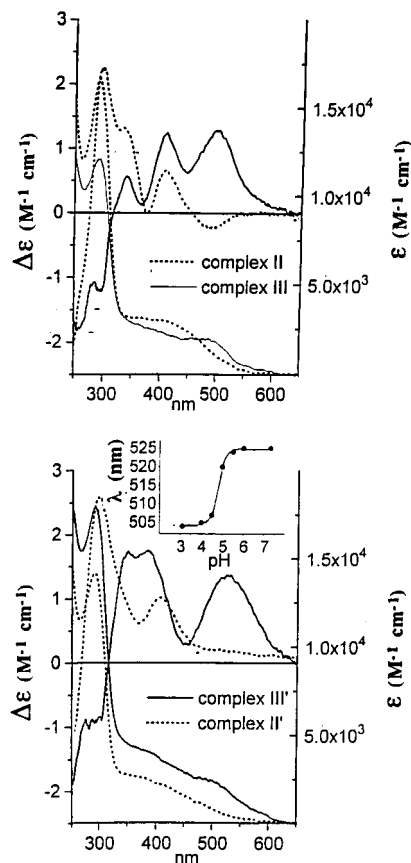


Figure 2. Absorption and CD spectra of complexes II, II', III, and III'.

the bands due to $\pi \rightarrow \pi^*$ of pyrimidine and bithiazole could be observed at ~ 240 nm often mixed into a single band. As for the free drug, a decrease of the amplitude of the CD signal was observed when the pH increased.

It has been previously shown by Loeb et al.^{26,27} that the absorption spectrum of Fe^{II}BLM exhibits an envelope of transitions that can be resolved into five bands at ~ 550 , 490, 440, 390, and 350 nm. These bands have been assigned as Fe(II) $d_{\pi} \rightarrow$ pyrimidine π^* MLCT transitions. The bands observed in the range 350–440 nm in the spectra of Ru^{II}BLM might plausibly be Ru(II) $d_{\pi} \rightarrow$ pyrimidine π^* MLCT transitions. However, we have prepared a complex with L-histidine (His) according to the procedure given for BLM complexes. The binding of Ru(II) to His resulted in the formation of one charge-transfer band at 444 nm. Thus, the CD spectrum of complex II might suggest the presence of a CT transition between the imidazole ring nitrogen of imidazole and the metal ion.

Resonance Raman Spectra of Complexes II and II'

Resonance Raman spectroscopy has shown to be very useful and powerful in describing the metal ion binding sites in iron-bleomycin and related systems.²⁴ The usefulness of resonance Raman spectroscopy is that the modes that show resonance enhancement are associated with the excited chromophore. Thus, assignment of the modes enhanced by excitation of a transition centered on a ruthenium ion in Ru-BLM complexes may provide quite convincing information about the coordination of the metal ion in these species. To obtain enhancement from modes of each of the Ru-BLM complex, we chose 488 nm as the excitation wavelength for the resonance Raman measurements (as we will see below, this wavelength was used to optimize the resonance Raman modes associated with a new absorption band around 500 nm).

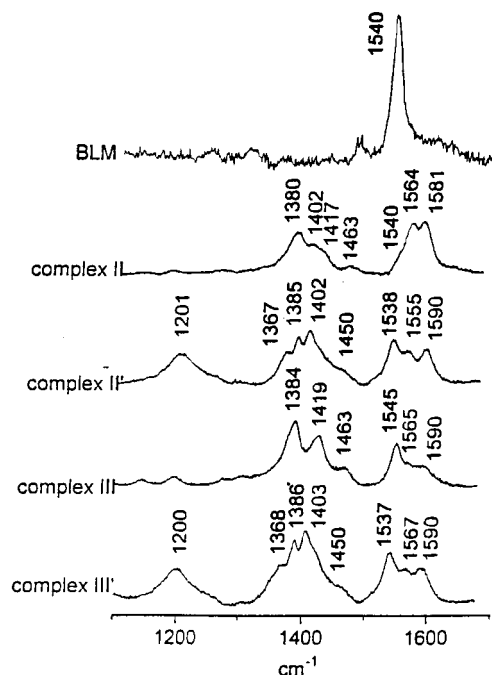


Figure 3. High-frequency region of the resonance Raman spectra of Ru(II)-BLM complexes II, II', III, and III'.

The nonresonant Raman spectrum of free BLM exhibited bands at 1543 cm^{-1} , which was previously assigned to the bithiazole moiety,²⁴ a very weak one at 1491 cm^{-1} , and another at 1386 cm^{-1} , which could be assigned to pyrimidine. In the resonance Raman spectrum of complex II, the nonresonant band of bithiazole at ~ 1540 cm^{-1} was still clearly seen and was used as the internal standard to indicate the relative intensities of the other bands (Figure 3). Additional bands that were not present in the spectrum of free BLM were seen at 1581 and 1564 cm^{-1} , and we assigned them to the amide I (C=O) and amide II (C-N) vibrations, respectively, for the following reason: in the absence of metal, the bands due to the amide I (C=O) and amide II (C-N) vibrations are usually localized at ~ 1660 and 1550 cm^{-1} , respectively. Through complexation with metal ion they shift to lower energy and higher energy, respectively. Then three bands (or shoulders) at 1463 , 1417 , and 1402 cm^{-1} were seen that might be assigned to imidazole vibrations, as well as the band at 1380 cm^{-1} that was already present in free BLM and was due to pyrimidine ring mode.²⁴

When the pH was increased from 4.0 to 7.0, the positions of these bands remained more or less the same; however, the intensities of the bands due to amide I and II vibration were decreased by a factor of 2. The most important modification was the appearance of a strong band at 1201 cm^{-1} . It is known that primary amine with secondary α -carbon absorbs weakly at ~ 1040 cm^{-1} and more strongly at 1140 – 1080 cm^{-1} .³⁵ This strongly suggested that this band was due to vibration of the α -amino group of the β -aminoalanine moiety, which at pH 7 would be bound to metal ion in apical position, as this occurs for Fe-BLM complex. No bands were detectable in the low-frequency region. It should be mentioned that all the above frequencies for complexes II and II' were insensitive to the H/D exchange; only small shifts were observed (± 1 – 4 cm^{-1}), which practically means that these vibrations did not involve exchangeable proton.

¹H NMR Spectra of Complex II. Complex II is diamagnetic, as concluded by EPR measurements and the line widths of the

(35) Rosado, M. T. S.; Duarte, M. L. R. S.; Fausto, R. *J. Mol. Struct.* **1997**, *410–411*, 343–348.

Table 2. Resonance Raman Spectral Features. Frequencies (cm⁻¹) of the Raman Lines for Ru–BLM (in H₂O) and Their Proposed Assignments^a

proposed assignment	II	II'	III	III'	BLM
amide I (C=O)	1581 (2)	1590 (0.8)	1590 (0.5)	1590 (0.5) sh	
amide II (C–N)	1564 (2)	1555 (0.8)	1565 (0.5) sh	1567 (0.5) sh	
bithiazole	1540 (1) sh	1538 (1)	1545 (1)	1537 (1)	1543 (1)
imidazole	1463 (0.25)	1450 (0.3) sh	1463 (0.3)	1450 (0.3) sh	
imidazole	1417 (1) sh		1419 (1)		
imidazole	1402 (1)	1402 (1.2)		1403 (1.1)	
pyrimidine					1491 (0.1)
pyrimidine	1380 (1.7)	1385 (1.1)	1384 (1.2)	1386 (1)	1386 (0.1)
pyrimidine		1367		1368	
α-amino of β-aminoalanine		1201 (0.8)		1200 (1)	
Ru–O			625 (0.1)	615(0.3)	
Ru–O			597 (0.2)	590 (0.5)	

^a Values in parentheses indicate the relative intensity of the bands using that of the nonresonant band of bithiazole as an internal standard.

peaks in the ¹H NMR spectrum. To assign the ¹H NMR spectrum of complex II, we first assigned the ¹H NMR spectrum of BLM at the same pH = 3.5 using a ¹H–¹H COSY sequence. The assignment for the ¹H NMR of BLM at pH = 3.5 was based on its previously assigned spectrum at pH = 4.0 by Haasnoot et al.³⁶ and on its protons' pH dependence studied by Chen.³⁷ Afterward, the ¹H NMR of complex II was assigned using its COSY ¹H–¹H spectrum and by direct comparison with the BLMs already assigned spectrum.

The biggest single peak in the spectrum of complex II (at 2.74 ppm), which increases as the reaction progresses, is assigned to the methyl protons of free DMSO.³¹ DMSO is gradually released from the starting complex RuCl₂(DMSO)₄, as BLM binds to ruthenium. As the formation of complex II takes place, the peak corresponding to the pyrimidine methyl group of metal-free BLM gradually disappears, and at the same time a new single peak near by the Sul Me peak appears at 2.98 ppm. The only candidate for this new peak is the Pyr Me protons of complex II.

Table 3 shows the positions for the assigned protons for complex II and BLM at pH = 3.5. As can be seen, the positions of protons of the Bit, Val, Thr, and Sul do not change significantly upon complexation. Therefore, it is assumed that these domains are not involved in the metal ion binding site. On the contrary, the following protons are shifted compared to free BLM: the His 2, His 4 of the imidazole ring; the His α, His β of the histidine moiety; the Pro α, α', β, and Pyr Me of the pyrimidyl propionamide and amino alanine moieties, respectively, and the Gul 1 proton of the gulose sugar. We can assume that these domains are coordinated to ruthenium. The specific binding sites for these moieties were derived by comparing our data to that of other NMR studies on various metallobleomycins that appeared in the literature.^{38–41}

More specifically, the His 2 protons' shift is greater than the His 4 shift, indicating that the complexation is done by the N3 of the ring. If complexation were through N5, one would expect the shifts for its neighboring protons to be of equal magnitude, which is not the case. The shifting of His α and His β protons is indicative of the histidine amide binding to the metal.

Table 3. ¹H NMR Chemical Shifts of Ru^{II}BLM Complexes (II and III) at 25 °C, in D₂O^a

	BLM (pH = 3.5)	complex II	complex III
Ala α	4.16	4.36	4.69
Ala β, β'	3.07	3.38	4.02
Bit α	3.28	3.29	3.29
Bit β	3.66	3.67	3.66
Bit 5	8.24	8.23	8.23
Bit 5'	8.07	8.06	8.06
Gul 1	5.30	5.34	5.34
Gul 2	4.11	4.12	4.12
His α	5.11	5.14	5.15
His β	5.52	5.59	5.60
His 2	8.75	8.81	8.79
His 4	7.62	7.64	7.60
Man 1	5.06	5.06	5.06
Man 2	4.06	4.08	4.09
Pro α, α'	2.67	2.92	3.17
Pro β	4.04	4.32	4.67
Pyr Me	2.03	2.98	—
Sul β	2.21	2.22	2.21
Sul α	3.42	3.41	3.41
Sul γ	3.64	3.63	3.64
Sul Me	2.95	2.96	2.96
Thr α	4.26	4.26	4.24
Thr β	4.09	4.10	4.10
Thr Me	1.14	1.12	1.13
Val α	2.60	2.61	2.61
Val β	3.76	3.76	3.77
Val γ	3.95	3.94	3.95
Val α-Me	1.17	1.15	1.18
Val γ-Me	1.16	1.18	1.17
Free DMSO		2.74	2.74

^a Abbreviations: Ala, β-aminoalanine; Bit, bithiazole; Gul, α-L-gulose; His, β-hydroxyhistidine; Man, α-D-mannose; Pro, propionamide; Pir, pyrimidine; Sul, γ-aminopropyl dimethylsulfonium; Thr, threonine; Val, methyl valerate.

As seen in other metallobleomycins,^{38–41} the large downfield shifting of the Pyr Me protons indicates that N1 of the pyrimidine ring is complexed to the metal center. The shifting of the Pro α, α'–Pro β, Ala α–Ala β, β' protons implicates the secondary amine between them in the complexation. The primary amine of the aminoalanine moiety does not seem to be coordinated to the ruthenium. Extensive NMR studies^{38–41} on various metallobleomycins has shown that when the terminal amine of the aminoalanine is bound to the metal, then the protons Ala β, β'—having the same chemical shift in free BLM—are found to have different chemical shifts, due most probably to the five-membered chelate ring formed with the two amines. Moreover, the pK_a of this terminal amine in free BLM is 7.5,²³ and it does not seem probable to be deprotonated for complexation at pH = 3.5.

(36) Haasnoot, G. A. G.; Pandit, U. K.; Kruk, C.; Hilbers, C. W. *J. Biomol. Struct. Dyn.* **1984**, *2*, 449–467.

(37) Chen, D. M.; Hawkins, B. L.; Glickson, J. *Biochemistry* **1977**, *16*, 2731–2738.

(38) Wu, W.; Vanderwall, D. E.; Lui, S. M.; Tang, X.; Turner, C. J.; Kozarih, J. W.; Stubbe, J. *J. Am. Chem. Soc.* **1996**, *118*, 1268–1280.

(39) Xu, R. X.; Nettesheim, D.; Otvos, J. D.; Petering, D. H. *Biochemistry* **1994**, *33*, 907–916.

(40) Oppenheimer, J. J. *Biochemistry* **1985**, *24*, 81–92.

(41) Akkerman, M. A.; Haasnoot, C. A. G.; Hilbers, C. W. *Eur. J. Biochem.* **1988**, *173*, 211–225.

Finally, the shifting of the Gul 1 proton seems to derive simply by a conformational change of this sugar due to the overall complexation of BLM. This assumption is based on the fact that no one has ever implicated the gulose in the complexation.^{38–41} Thus we can conclude that the binding sites for ruthenium in complex II are the N1 of the pyrimidine ring, the N3 of the imidazole ring, the deprotonated amide of the histidine, and the secondary amine.

Electrospray Mass Spectrometry of Complex II. The ES-MS spectra for complex II at an intermediate time during its formation showed several m/z peaks corresponding to doubly and triply charged ions of the following molecular ions: $[\text{Ru}^{2+} + \text{BLM}^+]$, $[\text{Ru}^{2+} + \text{BLM}^+ + \text{DMSO}]$, $[\text{Ru}^{2+} + \text{DMSO} + \text{Cl}^- + \text{BLM}^+ + \text{H}^+]$, $[\text{Ru}^{2+} + \text{BLM}^+ + 2\text{DMSO} + \text{Cl}^-]$. Their isotopic distribution resembles the one expected for Ru-BLM complexes. The first ion to be formed, from the interaction of BLM with $\text{RuCl}_2(\text{DMSO})_4$, was, as expected, the one with two DMSOs and one Cl^- ³³ still bound to the ruthenium. The rest of the assigned peaks reveal that, as the reaction progresses, the rest of the DMSOs are released, leaving a Ru-BLM complex. Indeed the ES-MS spectra for complex II, at a much later time during its formation, showed practically the same m/z peaks (apart from the peak for $[\text{Ru}^{2+} + \text{BLM}^+ + 2\text{DMSO} + \text{Cl}^-]$, which was completely missing), but this time, the peak corresponding to the molecular ion $[\text{Ru}^{2+} + \text{BLM}^+]$ was larger than the rest. The peaks corresponding to free BLM are barely visible, indicating that after a proper reaction time practically all BLM undergoes reaction with Ru(II). We can therefore conclude that the interaction of BLM with $\text{RuCl}_2(\text{DMSO})_4$ begins with the formation of a $\text{Ru}(\text{BLM})\text{Cl}(\text{DMSO})_2$ complex, then the bound BLM displaces the rest of the DMSOs, forming a Ru-BLM complex, which is complex II.² Complex II should contain Cl^- , because its CD spectrum is slightly different from that obtained using $\text{RuBr}_2(\text{DMSO})_4$ instead of $\text{RuCl}_2(\text{DMSO})_4$ as starting material. However, the spectral features of complex III (see below) are the same whether $\text{RuCl}_2(\text{DMSO})_4$ or $\text{RuBr}_2(\text{DMSO})_4$ is used.

Reaction of Ru(II)-BLM with O_2 , H_2O_2 , and PhIO. Complexes hereafter named III and III', depending whether the reaction was performed at pH 4.0 or 7.0, respectively, were prepared by three independent routes: the interaction of Ru(II)-BLM precursor (i) with dioxygen, (ii) with H_2O_2 , or (iii) with PhIO or pyridine *N*-oxide (see the reaction scheme).

Reaction of Ru(II)-BLM with Molecular Oxygen. When complexes II or II' are heated in the presence of oxygen (~1–2 h at 90 °C), they are converted to complexes III and III', respectively. Their formation was also monitored using absorption and CD spectroscopy. Actually, complex III was very rapidly and reversibly converted to complex III' just by increasing the pH from 4.0 to 7.0.

Reaction of Ru(II)-BLM with H_2O_2 . Both complexes can be very rapidly obtained by addition, at room temperature, of H_2O_2 to Ru(II)-BLM.

Reaction of Ru(II)-BLM with Iodosylbenzene. For two decades, researchers have used iodosylbenzene as a "single oxygen atom donor". The reaction between Ru(II)-BLM and PhIO, performed at room temperature, was very fast. One equivalent of PhIO was sufficient to ensure the total reaction.

As we have checked spectroscopically, the three reactions led to exactly the same dark orange compound, which was very robust and inert and could be kept for months without any special precaution.

Spectroscopic Characterization of Complexes III and III'. Both complexes were diamagnetic. Their formation was char-

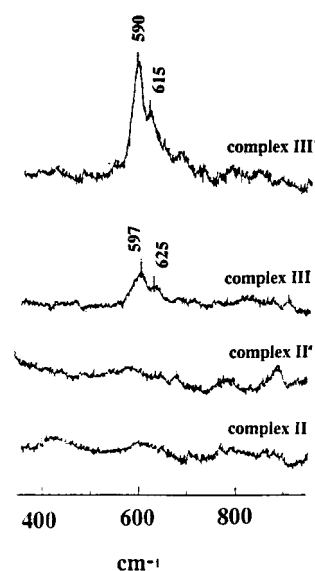


Figure 4. Low-frequency region of the resonance Raman spectra of Ru(II)-BLM complexes II, II', III, and III'.

acterized by the appearance of a positive band in the CD spectrum at 498 nm for complex III, which shifted to 526 nm for complex III' (Figure 2). Also in the absorption spectra a distinct band of CT origin was observed at the low-energy side (~500 nm) of the former broad CT transitions band. The other bands of the CD spectra were very close to those observed in complex II and II'. Complex III was reversibly converted to III' by increasing the pH from 4.0 to 7.0. The pK_a value of this reversible conversion calculated from spectrophotometric data (Figure 2, inset) was 4.8, which was very close to that observed for the high to low spin conversion of the iron(III)-BLM complex when the α -amino group of β -aminoalane binds to iron in an apical position.¹⁸ It should be noticed that the CD band at ~290 nm assigned to bithiazole was now negative.

In the high-frequency region the Raman spectra of complexes III and III' were very similar to those of complexes II and II', respectively (Figure 3). It should be emphasized that here also the conversion of complex III to III', through increase of the pH, yielded the appearance of a strong band at 1200 cm^{-1} . The low-frequency region (Figure 4) was characterized by the appearance of two bands around 600 cm^{-1} that we assigned, as will be discussed later, to Ru-O vibrations. This hypothesis was supported further by the fact that these bands were very weak when the laser line at 440 nm was used, i.e., when there was little contribution of 500-nm absorption (data not shown).

Discussion

The data discussed above show that in the absence of oxygen atom donor, BLM reacts with ruthenium, forming a 1:1 Ru(II)-BLM complex in which, according to our spectral data, the most likely ligands are the secondary amine nitrogen, the pyrimidine ring nitrogen, the deprotonated peptide nitrogen of the histidine residue, and the histidine imidazole nitrogen, coordinated as the basal planar donor, and the α -amino nitrogen of β -aminoalanine, coordinated as the axial donor at pH 7. The NMR spectra indicate also that complex II may not contain any DMSO molecule in its coordination sphere. This agrees with the results obtained from ES-MS. This coordination set is the same as that proposed for Fe(II)-BLM and most of metallobleomycins.³

Let us consider now the reaction of Ru(II)-BLM with molecular oxygen. We were expecting to observe reactions more

or less comparable to those observed when Fe(II)–BLM reacts with oxygen. Actually, Fe(II)–BLM plus O_2^- (in vitro) yields oxygenated BLM (O_2^- -Fe(II)–BLM or O_2^- -Fe(III)–BLM),^{15,42,43} a high spin, EPR silent Fe(III) species. This undergoes a disproportionation in which the oxidized product is O_2 plus Fe(III)–BLM, and the reduced product is activated bleomycin, a peroxide–Fe(III)–BLM complex.^{11,12,42,43} This breaks down with peroxide cleavage.³ According to resonance Raman data,²⁴ Fe(III)–BLM is liganded with OH^- liganded in the sixth position. Our data show that the reaction of Ru(II)–BLM with oxygen is different than that found for the iron complex. The same final very stable orange product is formed when starting complex (II or II') is reacting with molecular oxygen, or H_2O_2 , or PhIO. As the latter species is a donor of a single atom, this experiment indicates that only a single atom is bound to the ruthenium ion. The formation of the monomeric Ru(IV)–oxo species as the final product of Ru(II)–BLM oxidation is, however, unlikely. As mentioned above, the final product is very stable and does not oxidize DNA (data not shown), while the monomeric Ru(IV)–O complexes are very reactive and oxidize DNA or other organic molecules very effectively.^{44–46}

At this stage it is interesting to compare metallobleomycins with metalloporphyrins. It has been pointed out that in BLM, the β -hydroxyhistidine amide is conjugated to the pyrimidine ring and that one can speculate that together they comprise a delocalized π -electron buffer similar in function to the electron-buffering capabilities of the porphyrins.²⁶ Therefore, a suitable delocalized π -electron system, analogous to that in iron porphyrins, has been proposed for iron–BLM. Let us consider now Ru(II)–porphyrin. Some years ago, Collman et al.⁴⁷ synthesized a series of complexes $[Ru(IV)-(Por)X]_2O$, where X is an anionic ligand. They were obtained by oxidation of Ru(II)–porphyrin with molecular oxygen, and according to the authors, the reaction was striking. These complexes are diamagnetic, very robust, and kinetically inert. The interaction of Ru(II)–BLM with oxygen donor atom yielding a diamagnetic very robust and inert complex strongly reminded us of the behavior of these Ru(II)–porphyrins and suggests that complex III (III') might be formulated as $[Ru(IV)-BLM]_2O$. Another interesting point in our data is the observation that, if we make abstraction of the band at 500 nm in the visible spectrum and of the bands at $\sim 600\text{ cm}^{-1}$ in the resonance Raman spectra, which are characteristic of complex III, the modifications of the other bands, when going from complex II to III (or II' to III'), are very little, hardly suggesting that the electron density around Ru has not been greatly modified. It is worthwhile to be

reminded that molecular orbital calculations on the iron–porphyrin system demonstrate that the porphyrin macrocycle donates and withdraws electrons to the ferric and from the ferrous iron atom, respectively, to make the electron density on the iron invariant.⁴⁸ If this applies for Ru–porphyrin and by extrapolation to Ru–BLM, similar electron density around Ru in complex II and III might be expected.

Under these conditions it is tempting to assign the $\sim 600\text{ cm}^{-1}$ feature to the Ru–O–Ru stretch. However, on the basis of the observation that the $\nu_s(Fe-O-Fe)$ vibration of the μ -oxo dimer (TPP)–Fe–O–Fe–(TPP) has been detected at 366 nm,⁴⁹ the $\nu_s(Ru-O-Ru)$ vibration for Ru–O–Ru species are anticipated at significantly lower energy ($350\text{--}450\text{ cm}^{-1}$).⁵⁰ The unexpectedly high energy observed for the Ru–O–Ru vibration in the BLM complex could reflect a strong Ru–O bond. Actually, the structural characterization of the diamagnetic complex $K_4[(RuCl_5)_2O] \cdot H_2O$,⁵¹ the first Ru(IV)– μ -oxo complex to be reported, showed that the Ru–O–Ru bridge is linear and that the Ru–O bond length is shorter than expected for a Ru–O single bond. It is tempting also to assign the band that appears in the visible spectra at $\sim 500\text{ nm}$ to the CT transition between the Ru and oxygen atom. However, here also an oxo \rightarrow Ru(IV) charge transfer transition is anticipated at higher energy. It is likely, on the other hand, that the oxygen bridge may not be linear. As was shown by Sanders-Loehr et al., the bending of the oxygen bridge shifts the stretching vibration distinctly toward higher energy.⁵² Thus, the short Ru(IV)–O bond combined with the simultaneous bending of the oxygen bridge may have a distinct impact on the stretching vibration of the Ru–O–Ru unit.

Ru(II)–porphyrins with weakly coordinating axial ligands are spontaneously oxidized upon exposure to air. The sterically hindered porphyrin such as tetramesitylporphyrin Ru(II)–TMP(L)₂ afforded a *trans*-dioxoruthenium(VI) complex Ru(VI)–TMP(O)₂,⁵³ while in the case of sterically unhindered porphyrins, μ -oxo dimers of the type L–Ru(IV)–O–Ru(IV)–L have been reported.⁵⁴ The reaction of Ru(II)–BLM with oxygen is very similar to that of sterically unhindered Ru–porphyrins with oxygen.

Acknowledgment. This study was supported by the Centre National de la Recherche Scientifique, l'Université Paris Nord and a COST program.

IC001113M

- (42) Burger, R. M.; Kent, T. A.; Horwitz, S. B.; Munck, E.; Peisach, J. J. *Biol. Chem.* **1983**, *258*, 1559–1564.
 (43) Fulmer, P.; Petering, D. H. *Biochemistry* **1994**, *33*, 5319–5327.
 (44) Cheng, C.-C.; Goll, J. G.; Neyhart, G. A.; Welch, T. W.; Singh, P.; Thorp, H. H. *J. Am. Chem. Soc.* **1995**, *117*, 2970–2980.
 (45) Dovletoglou, A.; Adeyemi, S. A.; Meyer, T. *Inorg. Chem.* **1996**, *35*, 4120–4127.
 (46) Farrer, B. T.; Thorp, H. H. *Inorg. Chem.* **2000**, *39*, 44–49.
 (47) Collman, J. P.; Barnes, C. E.; Brothers, P. J.; Collins, T. J.; Ozawa, T.; Galluci, J. C.; Ibers, J. A. *J. Am. Chem. Soc.* **1984**, *106*, 5151–5163.

- (48) Zerner, M.; Gouterman, M.; Kobayashi, H. *Theor. Chim. Acta* **1966**, *6*, 363–400.
 (49) Burke, J. M.; Kincaid, J. R.; Spiro, T. G. *J. Am. Chem. Soc.* **1978**, *100*, 6077–6082.
 (50) Paeng, I. R.; Nakamoto, N. J. *J. Am. Chem. Soc.* **1990**, *112*, 3289–3297.
 (51) Mathieson, A. McL.; Mellor, D. P.; Stephenson, N. C. *Acta Crystallogr.* **1952**, *5*, 185–186.
 (52) Sanders-Loehr, J.; Wheeler, W. D.; Shiemke, A. K.; Averill, B. A.; Loehr, T. M. *J. Am. Chem. Soc.* **1989**, *111*, 8084–8093.
 (53) Groves, J. T.; Ahn, K.-H. *Inorg. Chem.* **1987**, *26*, 3833–3835.
 (54) Proniewicz, L. M.; Paeng, I. R.; Lewandowski, W.; Nakamoto, K. J. *Mol. Struct.* **1990**, *219*, 335–339.